Assessing the Flexural and Axial Behaviour of Reinforced Concrete Members at Elevated Temperatures Using Sectional Analysis

S.F. El-Fitiany, M.A. Youssef *

Department of Civil and Environmental Engineering, The University of Western Ontario, London, ON, Canada, N6A 5B9

Abstract

Simplified, rational, and practical models that account for effect of elevated temperatures on concrete and steel properties are needed. These models will enable engineers to design and assess Reinforced Concrete (RC) structures to satisfy specific fire performance criteria. This paper introduces a simple method that predicts the flexural and axial behaviour of RC sections during exposure to elevated temperatures. The method is based on using Finite Difference analysis to estimate the temperature distribution within a concrete section and a modified version of the well-known sectional analysis approach to predict the axial and/or flexural behaviour. A rational approach is proposed to convert the two-dimensional temperature distribution to one-dimensional distribution. This approach converts a complex problem to a simplified one and thus enables engineers to better understand the behaviour and have higher confidence in the results. The predictions of the proposed method are validated using experimental and analytical studies by others. Additional tests are needed to further validate and improve the proposed method.

Keywords: Reinforced concrete, fire, elevated temperature, flexural capacity, deformation, sectional analysis, curvature.

* Corresponding author: Tel.: +1 (519) 661-2111 x88661; fax: +1 (519) 661-3779.
E-mail address: youssef@uwo.ca

1. Introduction

Fire impacts Reinforced Concrete (RC) members by raising the temperature of the concrete mass. This rise in temperature dramatically reduces the mechanical properties of concrete and steel [1]. Moreover, fire temperatures induce new strains, thermal and transient creep [1]. They might also result in explosive spalling of surface pieces of concrete members [2].

Concrete structures are currently being designed for fire using prescribed methods that are based on experimental tests. These methods specify minimum cross-section dimensions and minimum clear cover to the reinforcing bars. As new codes are moving towards performance-based design and conducting experimental tests to satisfy different fire scenarios would be an expensive solution, engineers are in-need of new design tools to achieve specific performance criteria for a defined fire scenario. The Finite Element Method (FEM) has proven to be a powerful method to predict the behaviour concrete structures during exposure to fire events [3, 4]. Drawbacks of using the FEM, including the need to have a coupled thermal-stress analysis computer program and difficulty to comprehend its results and identify potential modelling errors, make it impractical for design engineers.

In this paper, a methodology that relies on using both Finite Difference Method (FDM) and a modified sectional analysis is proposed to estimate the behaviour of concrete sections during exposure to fire events. FDM is considered a simple method for evaluating the temperature variation within a concrete cross-section [5]. Sectional analysis allows evaluating the axial and/or flexural behaviour of a concrete section and is based on simple equilibrium and compatibility equations that can be easily applied by design engineers [6]. The modified sectional analysis is validated by comparing its predictions with the available experimental and analytical data.

The research conducted in this paper is limited to unprotected, siliceous, square concrete sections exposed to a standard ASTM-E119 fire from their four sides. This case is chosen since it

represents the general case of an interior concrete column in a typical building. Simple modifications can be introduced to address other cases and fire scenarios. Normal strength concrete is assumed and thus spalling is not considered [7].

The column tested by Lie et al. [8], Fig. 1a, is used in the following sections to provide example calculations for different components of the model. The column has dimensions of 305 mm by 305 mm and a height of 3810 mm. It is reinforced with 4-25 mm bars and has 10 mm ties spaced at 305 mm. The compressive and yield strength of the siliceous concrete and reinforcing bars are 36.1 and 443.7 MPa, respectively. The column is subjected to standard ASTM-E119 fire over a height of 3000 mm while being loaded axially.

2. Heat Transfer Model

Several methods are available to predict the temperature distribution in a concrete section due to exposure to fire temperatures. Simplified methods predict the temperature distribution using pre-assumed temperature variation [9, 10]. Such methods might produce accurate predictions for specific cases but might also result in significant errors for other cases. The FEM [11] is considered to be the most accurate tool to predict the thermal distribution as it accounts for irregular cross-sections subjected to any pre-specified fire condition. The FDM [5] is a simplified version of the FEM. It has the advantage of accounting for irregular shapes with good accuracy in addition to the ease of implementation in any programming code.

The following subsections briefly describe the required steps to predict the temperature gradient for a square, normal strength, siliceous concrete cross-section exposed to fire temperature from its four sides. A detailed description of the FDM is given by Lie [5]. The effect of steel reinforcement on the heat transfer calculations is neglected because of its small area relative to concrete area [5].

2.1. Concrete Thermal Properties

The amount of the heat transferred through the concrete mass is governed by its thermal conductivity (k_c) and specific heat capacity (C_c). For normal strength concrete, models representing k_c and C_c are reported by Lie [5].

2.2. Heat Transfer Mesh

The studied concrete section is divided into a number of 45 degree mesh elements as shown in Fig. 1b. The temperature at the centre of each element represents the temperature of the entire element. The location of any element inside the mesh can be determined from its coordinates and the mesh width ($\Delta\xi$), Fig. 1c.

2.3. Heat Transfer Calculations

Lie [5] proposed a set of equations that are based on the FDM to conduct heat transfer calculations. These equations are implemented into a C++ programming code. Fig. 2 shows a flowchart for the developed program. The boundary conditions including dimensions, number of exposed faces, and the fire duration are first identified. The incremental temperature increase at the surface of the column is determined at each time step based on the relationship between the fire temperature and its duration. Part of the heat energy conveyed to the boundary elements is used to increase their temperatures while the remaining energy is transferred to the inner elements. The effect of the moisture content is included based on the fact that water evaporates at a temperature of 100 ^{o}C [5]. As shown in Fig. 3, the relationship between the temperatures at points A, B, and C of the RC section and the fire duration predicted using the developed code is

in good agreement with the experimental results provided by Lie et al. [8]. Fig. 4a shows the temperature contours for the studied column after 1 hr of ASTM-E119 fire exposure.

3. Sectional Analysis

At ambient temperature, RC sections are analyzed using the well-known sectional analysis approach. For cases of single curvature, i.e. bending about horizontal axis, the concrete section is divided into horizontal discrete fibres as shown in Fig. 5. Utilizing the uniaxial stress-strain relationship for each fibre and taking into account equilibrium and kinematics, the mechanical behaviour of the section is analyzed. To simplify the analysis, two variables can be assumed; incremental centroidal axial strain, $\Delta\varepsilon_c$, and incremental curvature, $\Delta\psi$. Assuming a linear strain distribution, the incremental moment and axial force are obtained using Eq. (1).

$$\begin{pmatrix} \Delta M \\ \Delta P \end{pmatrix} = \begin{pmatrix} \sum_{i=1}^{n} E_i \times A_i \times y_i^2 & -\sum_{i=1}^{n} E_i \times A_i \times y_i \\ -\sum_{i=1}^{n} E_i \times A_i \times y_i & \sum_{i=1}^{n} E_i \times A_i \end{pmatrix} \times \begin{pmatrix} \Delta\psi \\ \Delta\varepsilon_c \end{pmatrix} \quad (1)$$

Where E_i is the modulus of elasticity of layer i, A_i is the area of layer i, y_i is the distance between the center of area of layer i and center of area of the cross-section.

For a given axial load, the moment-curvature behaviour is obtained in two stages. In the first stage, the axial strain is increased incrementally while curvature is kept equal to zero until reaching the required axial load. In the second stage, the axial load is kept constant and the applied curvature is increased. The corresponding change in the axial strain and the moment are calculated using Eq. (1). This process is repeated until reaching the required curvature value.

Applying sectional analysis to RC sections during exposure to elevated temperatures involves a number of challenges. The described sectional analysis is based on dividing the cross-section

into horizontal layers that have uniform properties. The temperature distribution within the cross-section width results in non-uniform properties. Section 3.2 proposes a method to divide the cross-section into layers with equivalent uniform properties. The second challenge results from the non-uniform thermal expansion within the cross-section depth. If the cross-section is free to expand, the total strain must be linear to satisfy the principle of plane sections which is still valid at elevated temperatures [12, 13]. The effective strain is thus non-uniform and the previously assumed linear distribution, Eq. (1), is no longer valid. Section 3.3 proposes a methodology to overcome this challenge.

Dwaikat and Kodur [14] used a two dimensional fibre model to analyze RC beams during fire exposure. The horizontal fibre model adopted in this paper is expected to provide better understanding of the behaviour at elevated temperatures as it converts a complicated two-dimensional fibre model to an equivalent one-dimensional fibre model.

3.1. Concrete and Steel Constitutive Models

As a preceding step to the analysis stage, the 45 degree mesh elements are modified to square mesh elements. The temperature at the center of each square element (m', n'), Fig. 1d, is taken as the average temperature of the adjacent 45 degree mesh elements. Based on the temperature reached in each square element, the mechanical properties of concrete and/or steel can be determined. Youssef and Moftah [1] provided an assessment of available constitutive models for concrete and steel at elevated temperatures. Based on this assessment, the models used in this paper are summarized in the following sub-sections.

3.1.1 Concrete compressive strength

Hertz model [15], Eq. (2), is used to predict the reduced concrete compressive strength (f'_{cT}). For loaded members, f'_{cT} should be increased by 25% [15].

$$f'_{cT} = \frac{f'_c}{1+\frac{T}{15,000}+\left(\frac{T}{800}\right)^2+\left(\frac{T}{570}\right)^8+\left(\frac{T}{100,000}\right)^{64}} \quad (2)$$

Where T is the temperature in degree Celsius, f'_c is the concrete compressive strength at ambient temperature.

3.1.2 Fire-induced strains

Total concrete strain at elevated temperatures (ε_{tot}) is composed of three terms: instantaneous stress related strain (ε_{fT}), unrestrained thermal strain (ε_{th}), and transient creep strain (ε_{tr}). The value of ε_{fT} at the peak stress (ε_{oT}) defines the stress-strain relationship during the heating stage and can be predicted using the model proposed by Terro [16], Eq. (3). For load level (λ_L) greater than 0.2, the effect of elevated temperatures on ε_{oT} can be neglected.

$$\varepsilon_{oT} = (50\lambda_L^2 - 15\lambda_L + 1)\,\varepsilon_{o1} + 20(\lambda_L - 5\lambda_L^2)\,\varepsilon_{o2} + 5(10\lambda_L^2 - \lambda_L)\times 0.002 \quad (3)$$

where $\varepsilon_{o1} = 2.05\times10^{-3} + 3.08\times10^{-6}T + 6.17\times10^{-9}T^2 + 6.58\times10^{-12}T^3$

$\varepsilon_{o2} = 2.03\times10^{-3} + 1.27\times10^{-6}T + 2.17\times10^{-9}T^2 + 1.64\times10^{-12}T^3$

ε_{th} is the free thermal strain resulting from fire temperature and can be predicted using the Eurocode model [17], Eq. (4).

$$\varepsilon_{th} = -1.8\times10^{-4} + 9\times10^{-6}\,(T-20) + 1.4\times10^{-11}\,(T-20)^3 \quad \le 12\times10^{-3} \quad (4)$$

ε_{tr} is induced during the first heating cycle of loaded concrete and is considered the largest component of the total strain. Due to the nature of experimental tests, ε_{tr} accounts for both the transient and creep components [1, 18]. Its value can be estimated using Terro's model [16].

$$\varepsilon_{tr} = \varepsilon_{0.3} \times \left(0.032 + 3.226 \frac{f_c}{f'_c} \right) \frac{V_a}{0.65} \quad (5)$$

Where

V_a is the volume fraction of aggregates

$\varepsilon_{0.3}$ is the transient creep strain for initial axial stress of $0.3\, f'_c$, and is given by Eq. (6)

$$\varepsilon_{0.3} = 43.87\times10^{-6} - 2.73\times10^{-8}\, T - 6.35\times10^{-8}\, T^2 + 2.19\times10^{-10}\, T^3 - 2.77\times10^{-13}\, T^4 \quad (6)$$

3.1.3 Initial modulus of elasticity

Concrete initial modulus of elasticity at ambient temperature, E_{ci}, is defined as the slope of the compressive stress-strain relationship at zero strain. Its value during heating, E_{ciT}, can be calculated using the model proposed by Anderberg and Thelandersson [19].

$$E_{ciT} = \frac{2 \times f'_{cT}}{\varepsilon_{oT}} \quad (7)$$

3.1.4 Concrete compressive stress-strain relationship

The model proposed by Youssef and Moftah [1] is adopted. The model includes simplified representation of transient creep strains. The relationship between the between the compressive stress, f_{cT}, and the corresponding compressive strain, ε_{cT}, is given by Eq. (8)

$$f_{cT} = f'_{cT} \left[2 \times \left(\frac{\varepsilon_{cT}}{\varepsilon_{oT} + \varepsilon_{tr}} \right) - \left(\frac{\varepsilon_{cT}}{\varepsilon_{oT} + \varepsilon_{tr}} \right)^2 \right] \qquad \varepsilon_{cT} \le \varepsilon_{oT} + \varepsilon_{tr} \quad (8.a)$$

$$f_{cT} = f'_{cT} \left[1 - Z\left(\varepsilon_{cT} - \varepsilon_{oT} - \varepsilon_{tr} \right) \right] \qquad \ge 0.2 \times f'_{cT} \qquad \varepsilon_{oT} \ge \varepsilon_{oT} \varepsilon_{tr} \quad (8.b)$$

Where Z is the slope of the descending branch of the concrete stress - strain relationship and is given by Eq. (8.c)

$$Z = \frac{0.5}{\frac{3+0.29f'_c}{145f'_c-1000}\times\frac{\varepsilon_{oT}}{\varepsilon_o}-\varepsilon_{oT}} \tag{8.c}$$

3.1.5 Reinforcing steel tensile stress-strain relationship

Lie's model [5] is used to predict the reduced yield strength of reinforcing bars f_{yT}, Eq. (9), and the stress-strain $(f_{sT}-\varepsilon_{sT})$ relationship, Eq. (10). The effect of creep of steel bars is found to have a minor effect on the behaviour of RC sections during fire exposure [4] and thus is not included in this study.

$$f_{yT} = \left[1+\frac{T}{900\times\ln\left(T/1750\right)}\right]\times f_y \qquad 0<T\le 600\ ^\circ\text{C} \tag{9.a}$$

$$= \left[\frac{340\text{-}0.34\times T}{T-240}\right]\times f_y \qquad 600<T\le 1000\ ^\circ\text{C} \tag{9.b}$$

$$f_{sT} = \frac{f(T,0.001)}{0.001}\times\varepsilon_{sT} \qquad \varepsilon_{sT}\le\varepsilon_p \tag{10.a}$$

$$f_{sT} = \frac{f(T,0.001)}{0.001}\varepsilon_p + f(T,[\varepsilon_{sT}-\varepsilon_p+0.001]) - f(T,0.001) \qquad \varepsilon_{sT}>\varepsilon_p \tag{10.b}$$

$$\varepsilon_p = 4\times10^{-6} f_y \tag{10.c}$$

$$f(T,0.001) = (50-0.04T)\times[1-e^{(-30+0.037T)\sqrt{0.001}}]\times 6.9 \tag{10.d}$$

3.2. Average Layer Temperature

The square mesh elements are grouped into horizontal fibres to conduct sectional analysis. This section presents a method to calculate equivalent temperatures for each fibre. These temperatures are used to estimate the concrete compressive strength, its modulus of elasticity, and transient creep and thermal strains.

To accurately predict the behaviour using sectional analysis, it is clear from Eq. (1) that the tangential modulus of elasticity is the most important factor thus it is proposed to estimate the average layer temperature such that it produces the average E_{ciT} for the square elements within the layer. This average temperature cannot be used to predict the thermal and transient creep strains as they are function of the element temperature, Eqs. (4) and (5). Instead, a second average layer temperature can be estimated using the algebraic average temperature of the square elements within the layer. Fig. 4b shows the distribution of two proposed average temperatures for the studied concrete section after one hour of exposure to ASTM-E119 standard fire.

The temperature of a steel bar can be assumed to be the same as the temperature of the square mesh element within which it is located. The variation of the temperature values over the cross-section height leads to different mechanical and thermal properties for each layer. Fig. 6a shows the estimated concrete stress-strain relationship at different elevated temperatures utilizing the model proposed by Youssef and Moftah [1]. Fig. 6b shows the stress-strain relationships for steel bars at different elevated temperatures utilizing the steel model presented by Lie [5].

3.3. Thermal and Effective Strain

Fig. 7a shows the expected linear distribution of total strains (ε_{tot}) due to an eccentric compression load P. This linear shape is based on the fact that plane sections remain plane after loading, which is still valid at elevated temperatures. Knowing the average temperature for each layer, concrete and steel thermal strains (ε_{th}) can be evaluated. The distribution along the height of the average ε_{th} for a square cross-section exposed to fire from its four sides is shown in Fig. 7a.

For unrestrained concrete sections, the effective strain (ε_{cT}) can be calculated by subtracting concrete and steel thermal strains from the total strain. The nonlinear distribution of thermal strains results in a nonlinear effective strain distribution, Fig. 7a. As Eq. (1) is only applicable for

linear strain distributions, the following sub-sections present a methodology to conduct sectional analysis for the non-linear varying effective strain distribution. If the concrete member is restrained, this method is not needed as ε_{cT} is equal to ε_{tot}.

3.3.1 Isolation of thermal strain component

Nonlinear thermal strains can be approximated to an equivalent linear distribution using a similar methodology to that proposed by Collins and Mitchell [12] and Tassios and Chronopoulos [13]. For the case of a square cross-section exposed to fire at its four sides, the thermal strain is expected to be symmetric as shown in Fig. 7a. The equivalent shape has a zero curvature and is defined by an axial strain ($\overline{\varepsilon_{th}}$), Fig. 7b. The value of $\overline{\varepsilon_{th}}$ is evaluated such that the axial forces in concrete and steel layers resulting from the difference between the actual thermal strain distribution and $\overline{\varepsilon_{th}}$ are in self equilibrium. An iterative procedure is used to calculate the value of $\overline{\varepsilon_{th}}$ such that the compressive force in concrete, C_{th}, is equal to the tensile force in the reinforcing steel bars, T_{th}. Concrete tensile strength is neglected.

Fig. 7c shows the nonlinear thermal strain distribution for the studied column after 1 hr standard ASTM-E119 fire exposure. Steel thermal strain is predicted for a temperature of 310 ^{o}C. The presented thermal strain distribution is converted to a linear distribution by considering section equilibrium. The equivalent uniform strain reflects the actual deformation of the concrete section. Differences between the non-linear and equivalent uniform strains represent concrete and steel stresses that are in equilibrium.

3.3.2 Thermally induced stresses:

The conversion from the actual nonlinear strain distribution to the equivalent linear distribution induces self-equilibrating internal strains ($\varepsilon_{\sigma th}$), Figs. 7b and 7c. These internal strains are part of mechanical strains required to retain the geometric linearity of the cross-section. To account for these strains, they are included as initial strains for each concrete and/or steel fibre.

3.4. Analysis Steps of RC Sections under Fire Loading

Figs. 8, 9, and 10 summarize the steps required to analyze RC sections during exposure to fire temperatures. The analysis can be divided into three main steps.

1. The heat transfer model is applied and the heat gradient through the cross-section is predicted. The average temperatures for each layer are then obtained.
2. The equivalent uniform thermal strain $\overline{\varepsilon_{th}}$ is then calculated by equilibrating the forces in the concrete and steel layers resulting from the actual thermal strain distribution. The difference between the actual and uniform strain distributions represents the induced strains $\varepsilon_{\sigma th}$ in concrete and steel layers to satisfy the section geometry. These strains are considered as initial strains in the following step.
3. Sectional analysis, Figs. 9 and 10, is conducted to construct the axial load-axial strain and moment-curvature diagrams.

3.4.1 Axial load–axial strain relationship

Fig. 11a shows the axial load–axial strain curves for the studied column prior to being exposed to fire and after 1 hour of exposure to standard ASTM-E119 fire. It is clear that fire

temperature reduced the compressive strength of the column by about 20% and increased strain values. Point A on the curve represents the expansion of the column under no external loads. The strain corresponding to this point represents the equivalent linear thermal strain ($\overline{\varepsilon_{th}}$). At point B, the stiffness of the section increases due to the elimination of the residual tensile stresses affecting the middle part of the concrete section. The compressive load at which the total strain is equal to zero is corresponding to point C. The axial capacity of the column is defined by point D.

3.4.2 Moment - curvature diagrams

Moment curvature curves represent the flexural behaviour of RC section under specified axial load level ($\lambda = f_c / f'_c$). Fig. 11b shows the effect of axial load level on the studied section prior and after 1 hr standard ASTM-E119 fire exposure. At elevated temperatures, λ affects the results in a similar manner to that observed at ambient temperature. Lowering λ from 1.0 (concentric load) to 0.4 (balance point) results in higher ductility accompanied with increase in the flexural capacity. Further reduction in the value of λ decreases the flexural capacity and increases the ductility.

4. Validation

The suggested methodology is validated by comparing its predictions with analytical and experimental data available in the literature.

4.1. Load Capacity Validation

The described sectional analysis methodology is applied on the column studied in the previous sections [12] and the axial load-axial strain relationships are constructed at different fire durations. The peak points of these curves represent the axial capacity of the studied column

during fire exposure. Fig. 12 shows good matching between the predictions of the proposed model, the experimental work, and the analytical work by Lie et al. [8]. The difference between the predictions by Lie et al. [8] and the proposed method is almost constant at all temperatures and thus is not related to the proposed method.

4.2. Axial Deformations

The column studied in the previous sections was fire tested while having an axial load of 800 kN and 1067 kN. The prescribed sectional analysis method is applied on the column cross-section and axial load-axial strain diagrams are constructed at specified fire durations. At any time during fire exposure, the axial deformation of the column is calculated by multiplying the axial strain corresponding to the applied axial load by the length of the column exposed to the fire. Figs. 13a and 13b show the axial deformation (u*)-time curves for the two columns. The initial expansion is due to the expansion of the concrete and steel materials. The subsequent gradual contraction happens when the material strength decreases significantly and the load effect becomes more pronounced. The predicted values have acceptable matching when compared with the experimental results by Lie et al. [12] and FEM analytical studies [4].

The same column cross-section was tested by Kodur et al. [20]. The total height of the column is 3.81 m while the length subjected to fire is 3.1 m. The concrete compressive strength is 40.2 MPa and the yield strength for reinforcing bars is 420 MPa. A preloading force P of 930 kN is applied prior to start of heating and kept constant during fire testing. From Fig. 13c, and given the complexity of the problem, a general acceptable agreement can be noticed between the predictions of sectional analysis method, FEM [3], and test results [20]. Differences between these three methods are mainly due to different predictions provided by different material models. This reason is supported by the work of Youssef and Moftah [1] which showed that

material models for concrete at elevated temperatures results in significantly different predictions. Even so the models used in this paper are those proposed by Youssef and Moftah [1] based on comparisons with experimental results, errors are still expected due to the complexity of the problem.

4.3. Lateral Deflection

Bratina et al. [4] analyzed a 4 m column subjected to a load of 930 kN at an eccentricity of 40 mm and exposed to Eurocode 1 standard fire [21] using FEM. The same column is analyzed using the proposed sectional analysis methodology. The moment-curvature diagrams are constructed at different fire durations. The lateral deflection w^* at each time step was estimated using the moment-area method for the estimated curvature distribution along the column height. Failure criteria proposed by BS 476 and adopted by Kodur and Dwaikat [22] are used. These criteria are setting limits for the maximum allowable deflection, Eq. (11), and maximum rate of deflection, Eq. (12).

$$\Delta_{max} = \frac{L}{20} \tag{11}$$

$$\left(\frac{\partial \Delta}{\partial t}\right)_{max} = \frac{L^2}{9000d} \quad \text{(mm/minute)} \tag{12}$$

Where L is the span between the supports (mm) and d is the effective depth of the beam (mm)

The analysis is conducted twice, ignoring and considering geometric nonlinearity. For each step, moment values along the column axis are magnified to account for the corresponding lateral deflection calculated in the previous time step. The obtained results are plotted in Fig. 14. An excellent matching is found between the sectional analysis and the FEM conducted by Bratina et al. [4] up to 90 minutes. However, the difference in predicting failure is about 15 minutes.

Differences between the predictions of sectional analysis and those of Bratina et al. [4] are due to the use of different material models and different failure criteria. Additional experimental work is required to further validate cases of eccentric loading. It is clear that ignoring geometric nonlinearity leads to underestimation of the lateral deformations. When geometric nonlinearity is considered, failure is predicted to occur at about 120 minutes due to reaching the limit given by Eq. (12). The proposed sectional analysis results in failure prediction which is almost matching the Eurocode 2 prediction [4, 21].

5. Summary and Conclusion

In this paper, a new simplified method that combines heat transfer and sectional analysis is developed. The Finite Difference Method is adopted to conduct heat transfer calculations due to its simplicity and accuracy. The traditional sectional analysis is modified to account for the effect of elevated temperatures. The paper is the first to propose conducting a one-dimensional sectional analysis, where the RC section is divided into horizontal fibres, to estimate the flexural and axial behaviour of RC sections during exposure to elevated temperatures. The success for such analysis relies on the average weighted temperature assigned for each fibre. To accurately predict the stiffness of each fibre, an average temperature based on achieving the average modulus of elasticity for that fibre is proposed. The algebraic average for temperatures of the elements forming the fibre is proposed to estimate the thermal strain and transient creep strain. The predictions of the proposed method are found to have relatively good agreement with experimental and analytical work by others. Additional tests are needed to further validate and improve the method for different concrete mixtures, aggregate types, fire scenarios, cross-section dimensions, number of exposed surfaces, and loading conditions. Extensive research is also

needed to utilize this method at the structure level which requires accounting for fire-induced deformations.

Acknowledgments

This research was funded by the Natural Sciences and Engineering Research Council of Canada (NSERC).

References

[1] Youssef, M.A. & Moftah, M. 2007, "General stress-strain relationship for concrete at elevated temperatures", Engineering Structures, vol. 29, no. 10, pp. 2618-2634.

[2] Khoury, G.A. 2000, "Effect of fire on concrete and concrete Structures", Progress in Structural Engineering and Materials, vol. 2, no. 4, pp. 429-447.

[3] Bratina, S., Saje, M., Planinc, I. 2007, "The effects of different strain contributions on the response of RC beams in fire", Engineering Structures, vol. 29, no. 3, pp. 418-430.

[4] Bratina, S., Cas, B., Saje, M., Planinc, I. 2005, "Numerical modelling of behaviour of reinforced concrete columns in fire and comparison with Eurocode 2", International Journal of Solids and Structures, vol. 42, no. 21-22, pp. 5715-5733.

[5] Lie, T.T. 1992, "Structural Fire Protection", ASCE Manuals and Reports on Engineering Practice, no. 78, New York, NY, USA, 241 pp.

[6] Youssef, M.A., Rahman, M. 2007, "Simplified seismic modelling of reinforced concrete flexural members", Magazine of Concrete Research, vol. 59, no. 9, pp. 639-649.

[7] Kodur, V.K.R., Sultan, M.A. 2003, "Effect of temperature on thermal properties of high-strength concrete", ASCE Journal of Materials in Civil Engineering, vol. 15, no. 2, pp. 101-107.

[8] Lie, T.T., Lin, T.D., Allen, D.E., Abrams, M.S. 1984, "Fire resistance of reinforced concrete columns", Technical Paper No. 378, Division of Building Research, National Research Council of Canada, Ottawa, ON, Canada.

[9] Wickstrom, U. 1986, "A very simple method for estimating temperature in fire exposed concrete structures", Fire Technology Technical report SP-RAPP 1986, 46, Swedish National Testing Institute, pp. 186-194.

[10] Malhotra, H.L. 1982, "Design of Fire-Resisting Structures", London, Surrey University Press, 226 pp.

[11] Lie, T.T. 1972, "Fire and Buildings", Applied Science Publishers Ltd, London, UK, 276 pp.

[12] Collins, M.P., Mitchell, D. 1987, “Prestressed Concrete Basics”, Canadian Prestress Concrete Institute, Ottawa, ON, Canada.

[13] Tassios, T.P., Chronopoulos, M.P. 1991, "Structural response of RC elements under fire", The Structural Engineer, vol. 69, no. 15, pp. 277-281.

[14] Dwaikat, M.B., Kodur, V.K.R. 2008, "A numerical approach for modeling the fire induced restraint effects in reinforced concrete beams", *Fire Safety Journal,* vol. 43, no. 4, pp. 291-307.

[15] Hertz, K.D. 2005, “Concrete Strength for Fire Safety Design”, Magazine of Concrete Research, vol. 57, no. 8, pp. 445-453.

[16] Terro, M.J. 1998, "Numerical modeling of the behavior of concrete structures in fire", ACI Structural Journal, vol. 95, no. 2, pp. 183-193.

[17] Eurocode 2, 1992, “Design of Concrete Structures”, ENV EC2.

[18] Fletcher, I.A., Welch, S., Torero, J.L., Carvel, R.O., Usmani, A. 2007, “Behaviour of concrete structures in fire”, Thermal Science, vol. 11, no. 2, pp. 37-52.

[19] Anderberg, Y, Thelandersson, S 1976, “Stress and deformation characteristics of concrete at high temperatures: 2 experimental investigation and material behaviour model”, Bulletin 54, Lund institute of Technology, Sweden.

[20] Kodur, V.K.R., Cheng, F., Wang, T., Sultan, M.A. 2003, "Effect of strength and fiber reinforcement on fire resistance of high-strength concrete columns", ASCE Journal of Structural Engineering, vol. 129, no. 2, pp. 253-259.

[21] Lennon, T., Moore, D.B., Wang, Y.C., Bailey, C.G. 2007, "Designers' guide to EN 1991-1-2, 1992-1-2, 1993-1-2 and 1994-1-2: handbook for the fire design of steel, composite and concrete structures to the Eurocodes", Thomas Telford, Reston, VA, 131 pp.

[22] Kodur, V.K.R., Dwaikat, M. 2007, "Performance-based fire safety design of reinforced concrete beams", Journal of Fire Protection Engineering, vol. 17, no. 4, pp. 293-320.

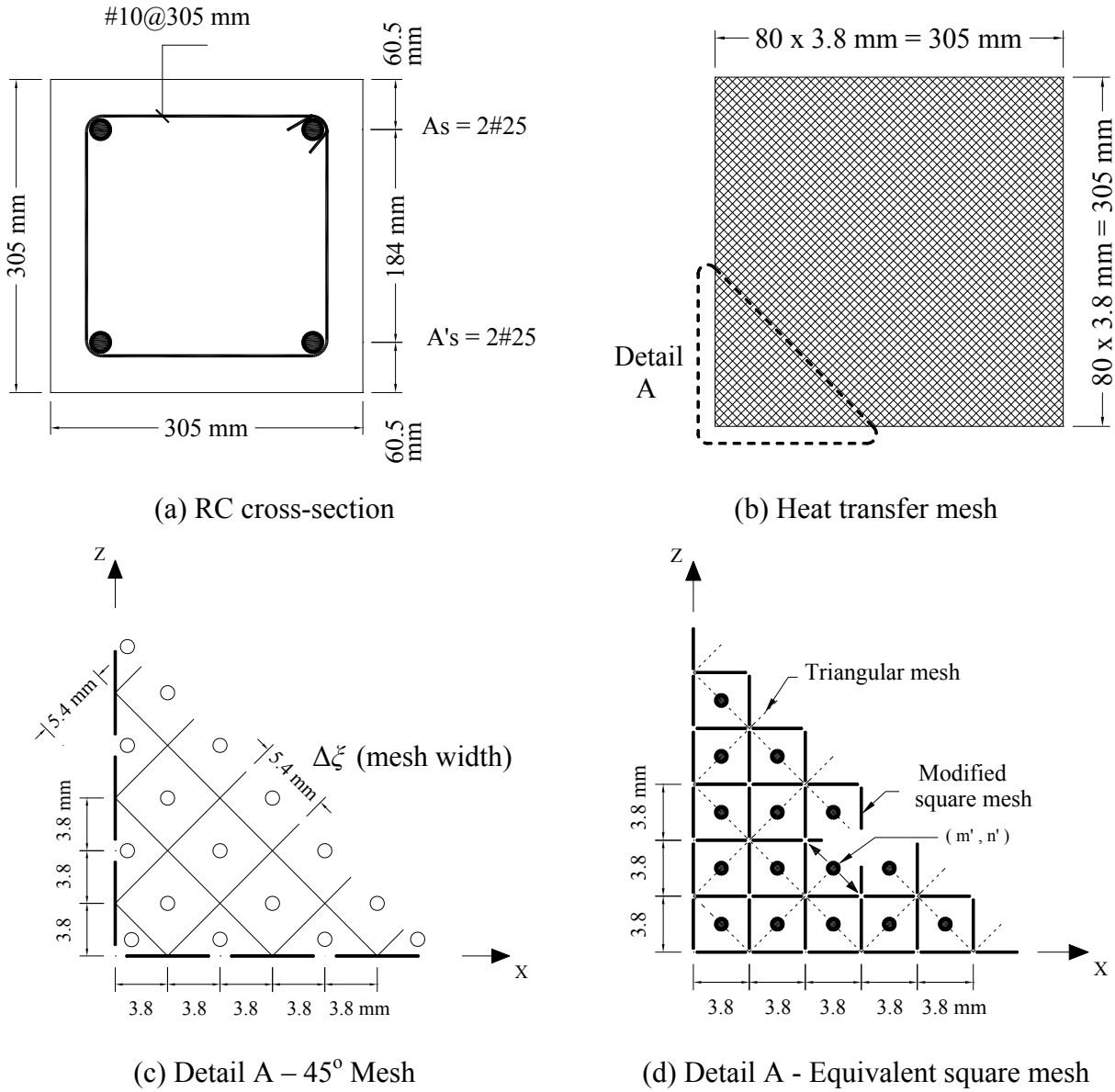

Fig. 1. Heat transfer modeling

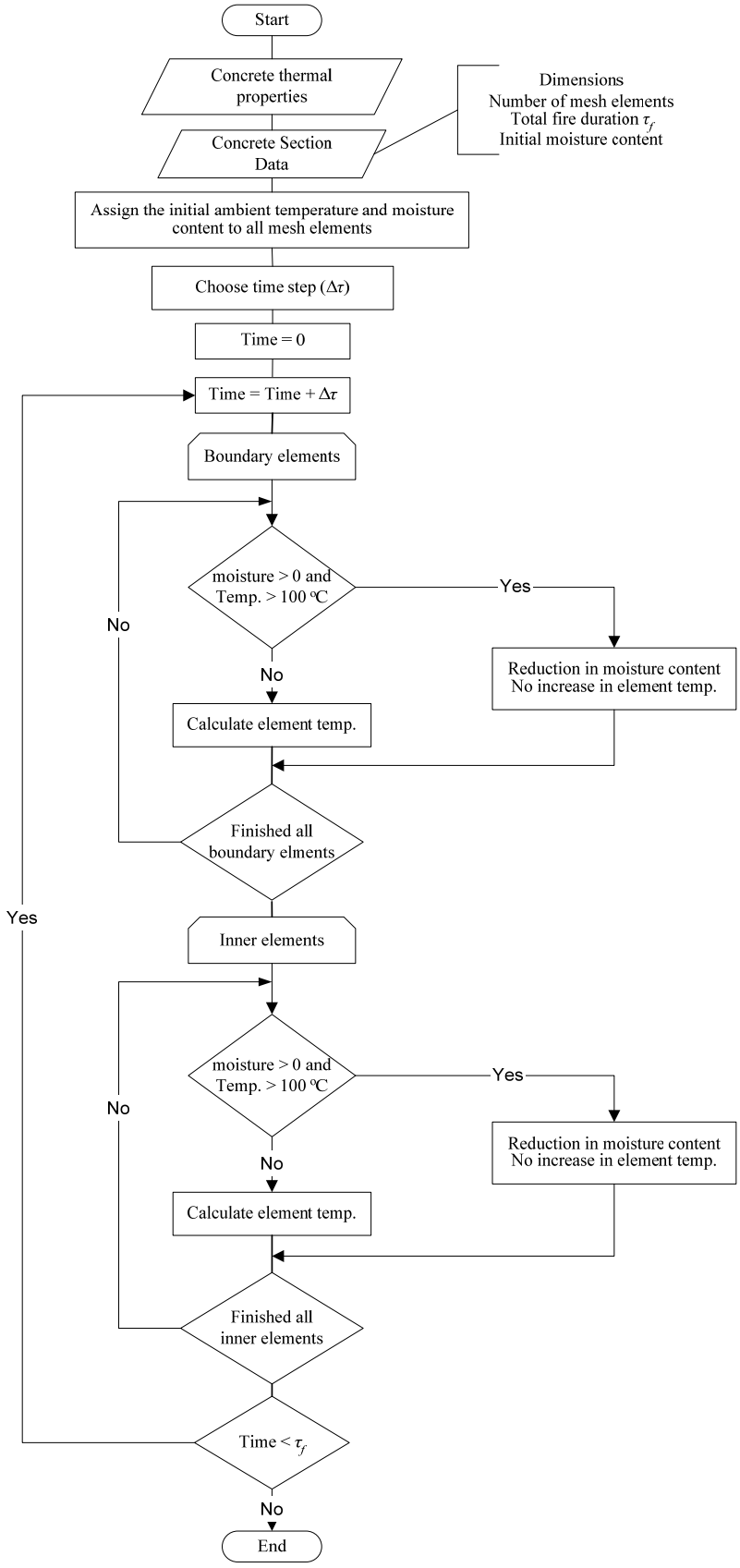

Fig. 2. Heat transfer analysis

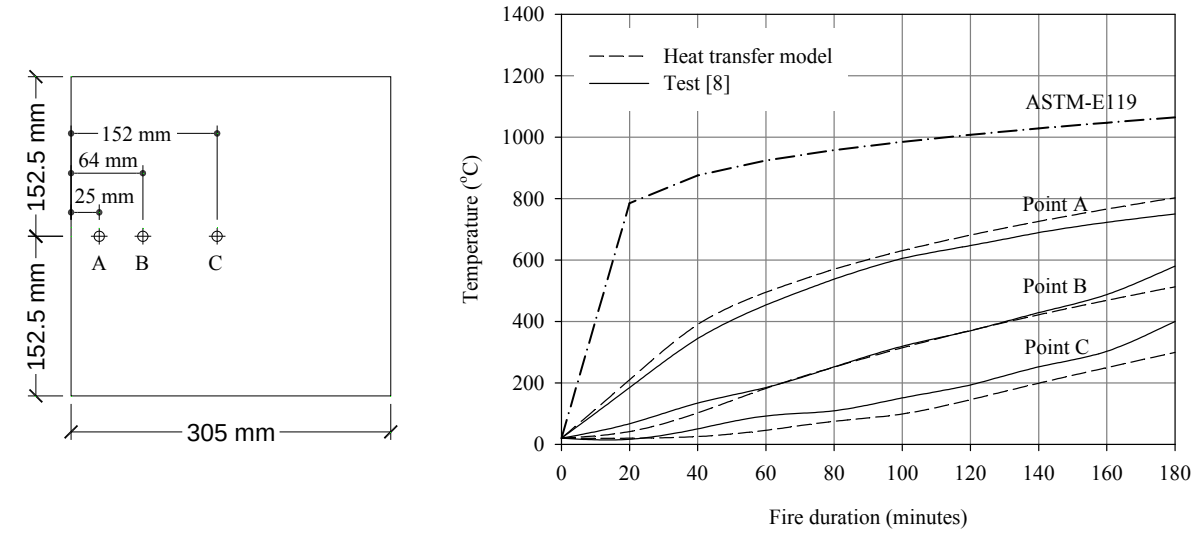

(a) Measurement locations (b) Temperature-fire duration relationship

Fig. 3. Validation of the heat transfer program

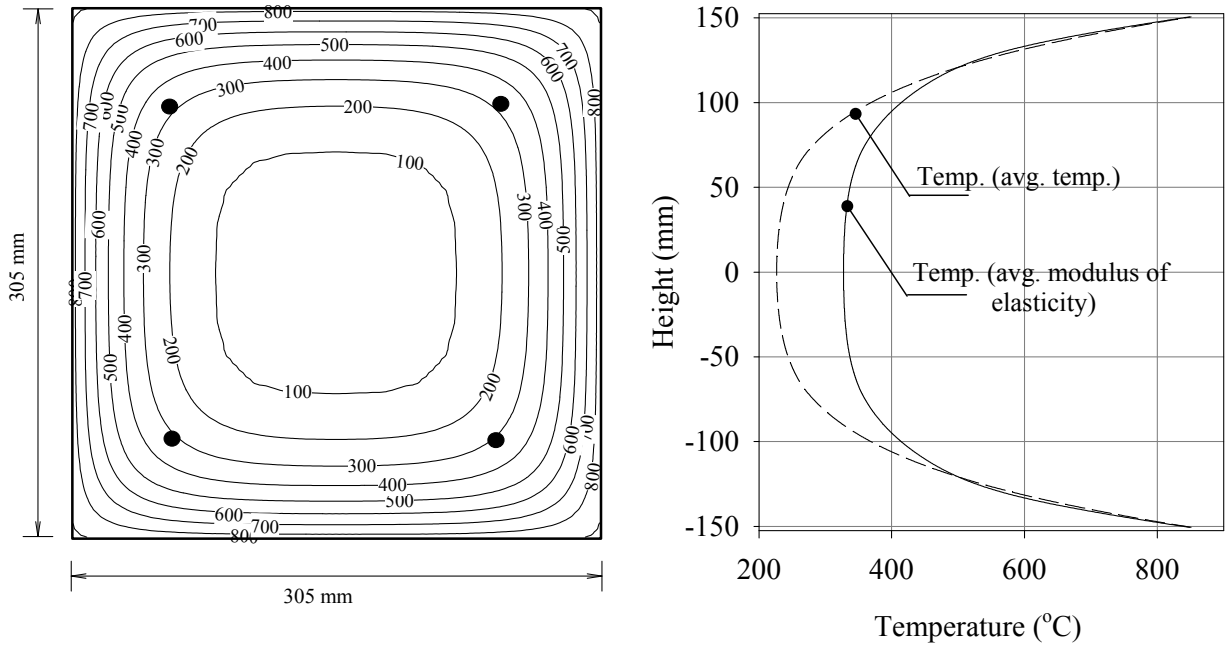

(a) Two-dimensional temperature distribution (°C)

(b) One-dimensional temperature distribution (°C)

Fig. 4. Temperature after 1 hr exposure to ASTM-E119

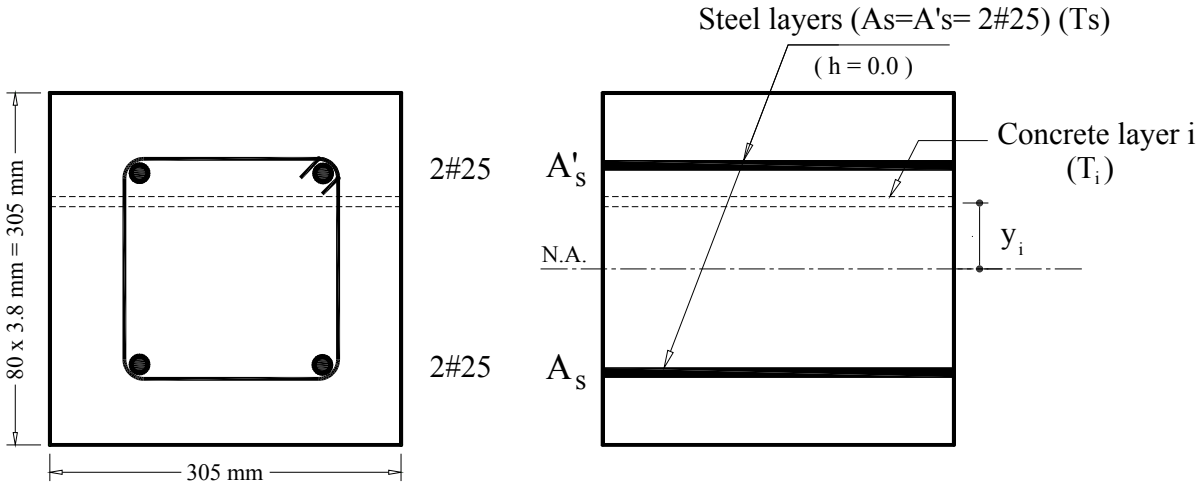

Fig. 5. Fibre model

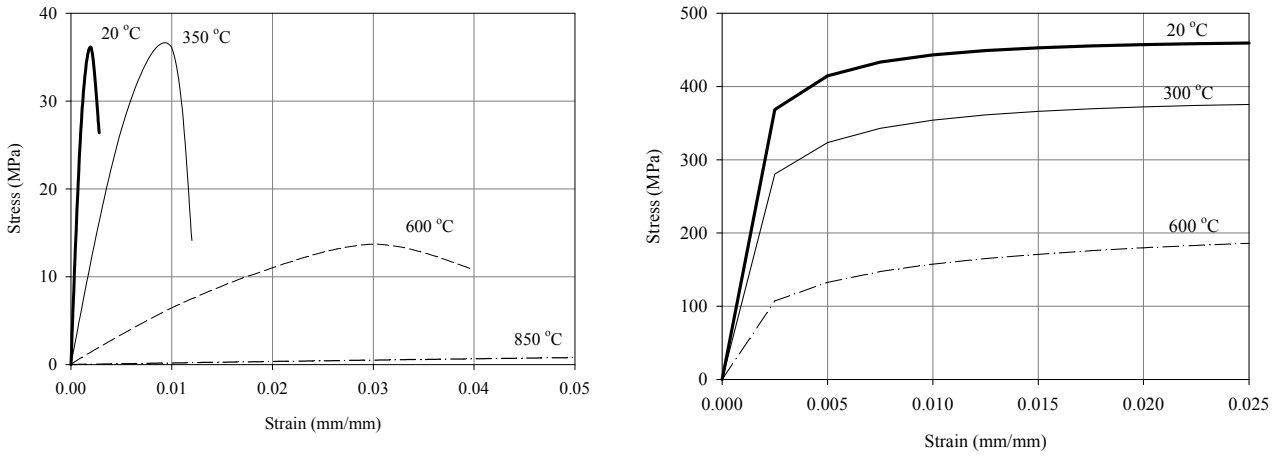

(a) Concrete in compression (b) Steel

Fig. 6. Stress-strain relationship at different temperatures

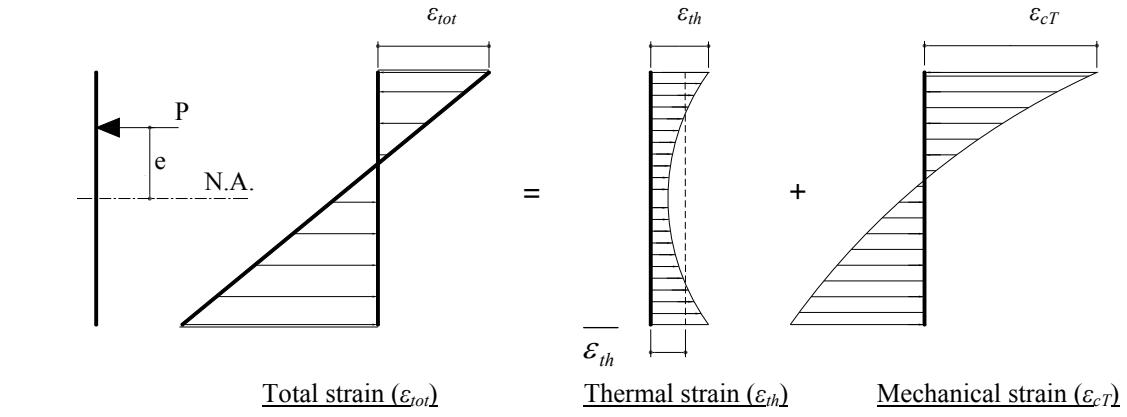

(a) Components of total strain

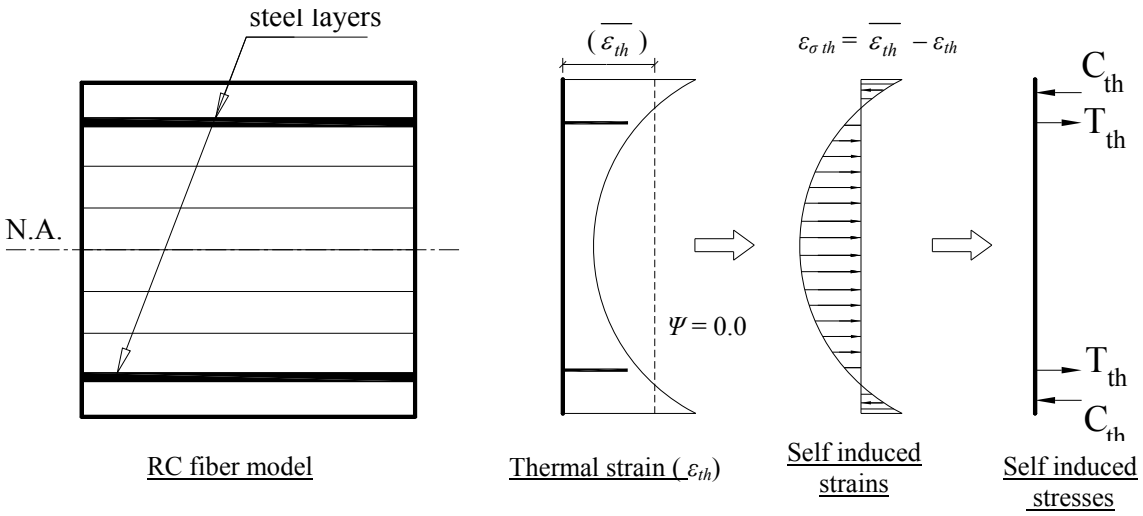

(b) Calculation of equivalent thermal strain

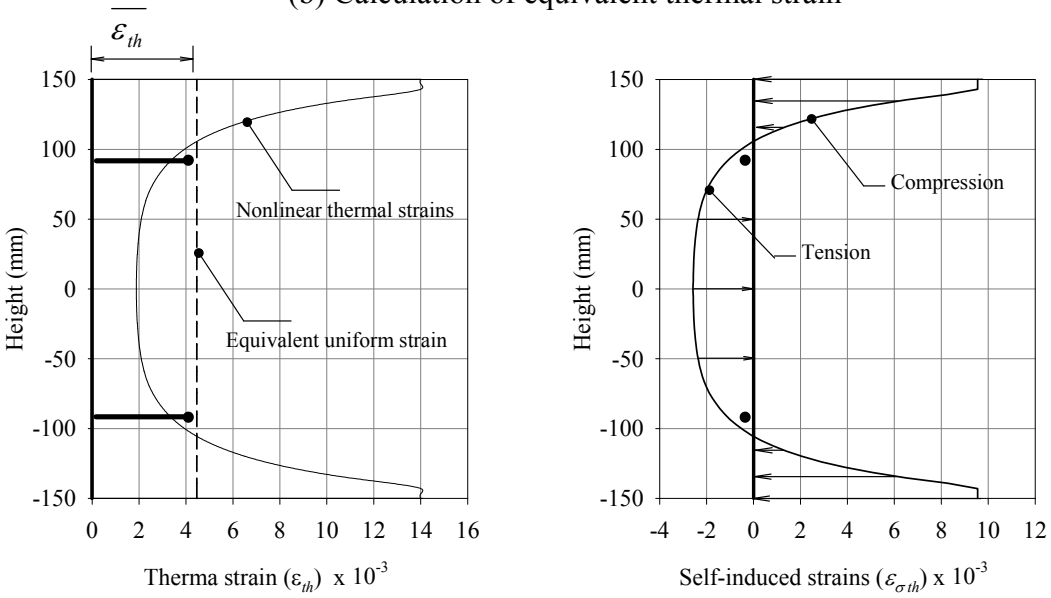

(c) Example calculation

Fig. 7. Effect of thermal strains on square RC sections exposed to fire from four sides

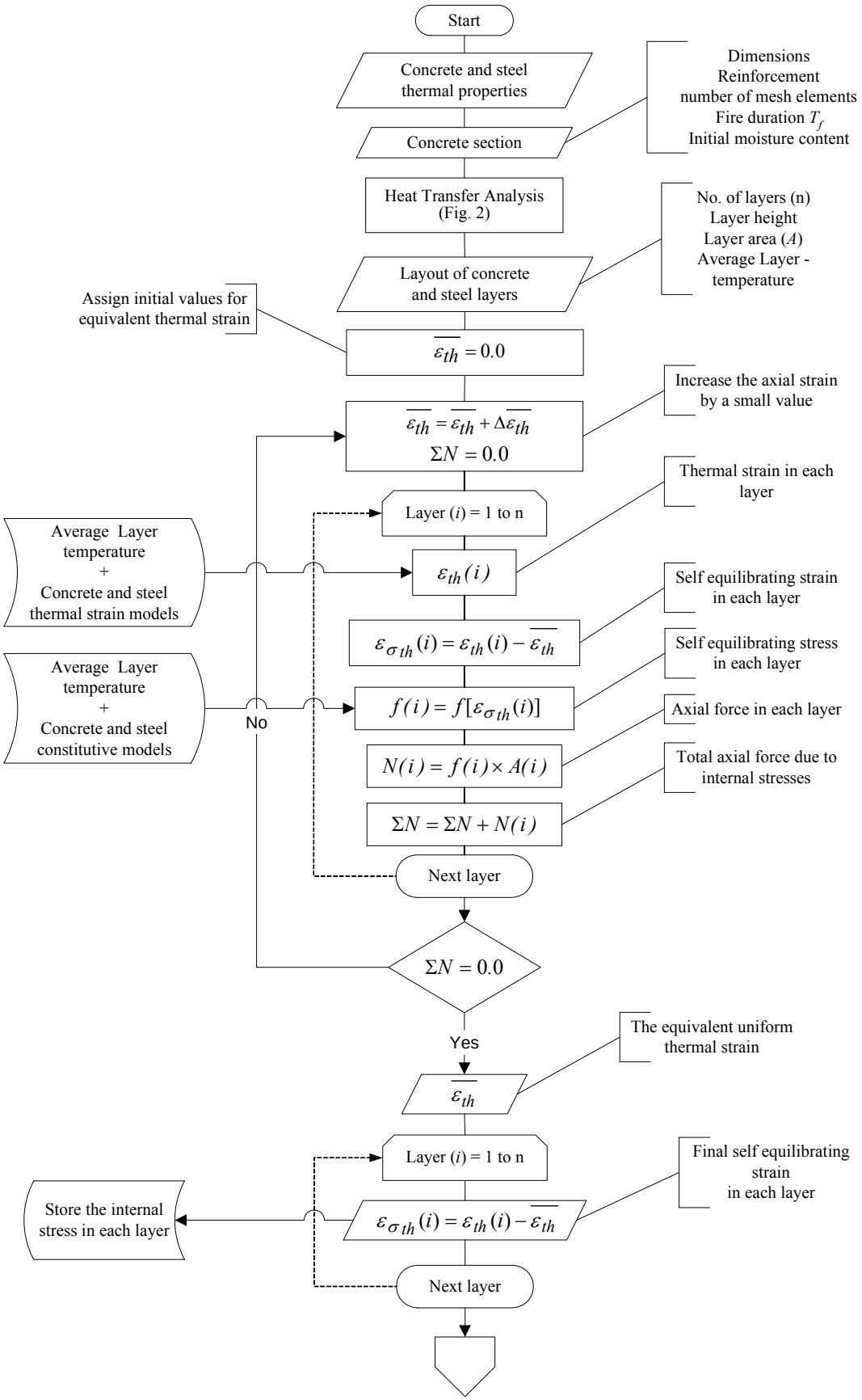

Fig. 8. Calculation of equivalent uniform thermal strains

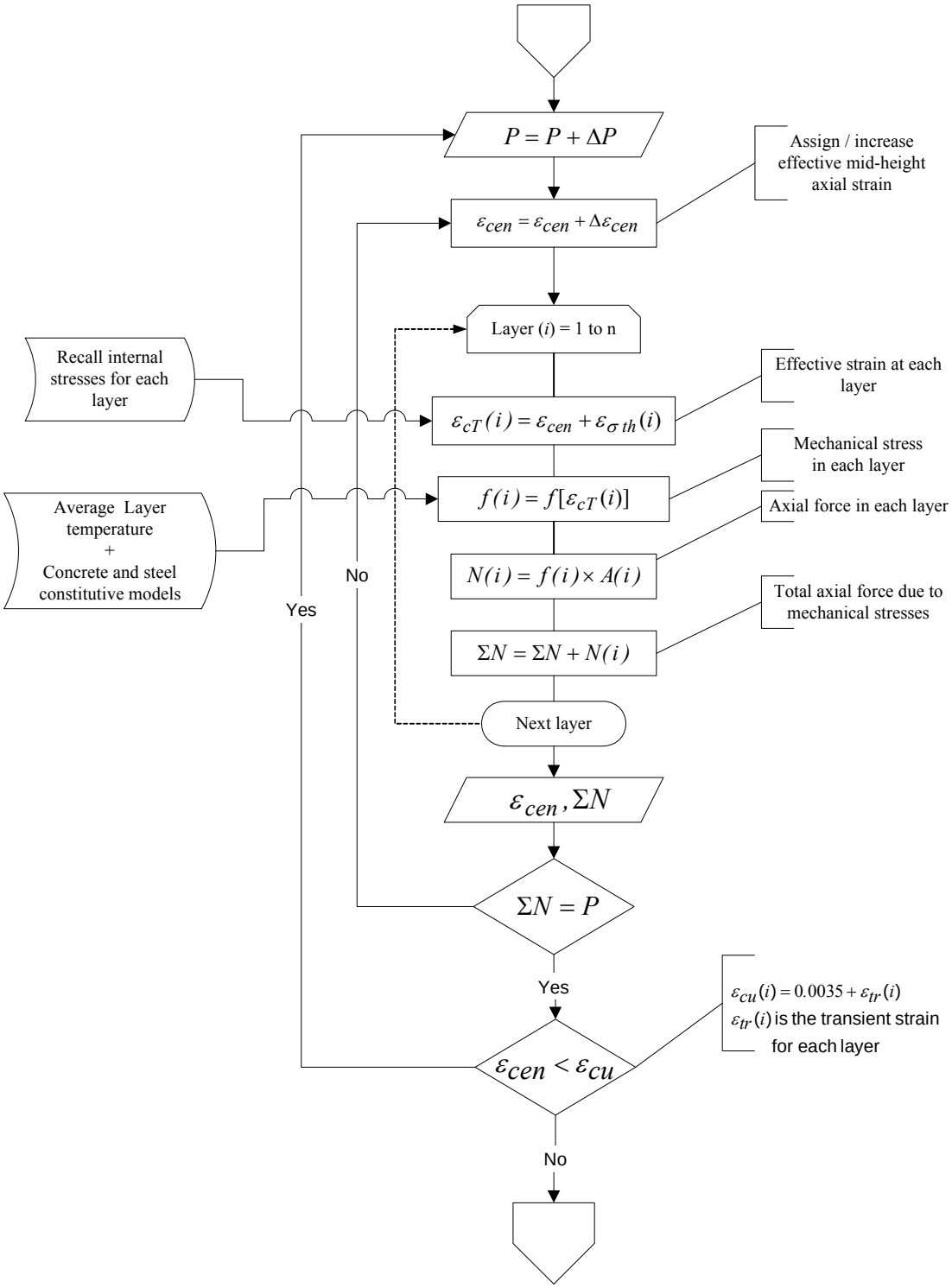

Fig. 9. Load-axial strain relationship construction

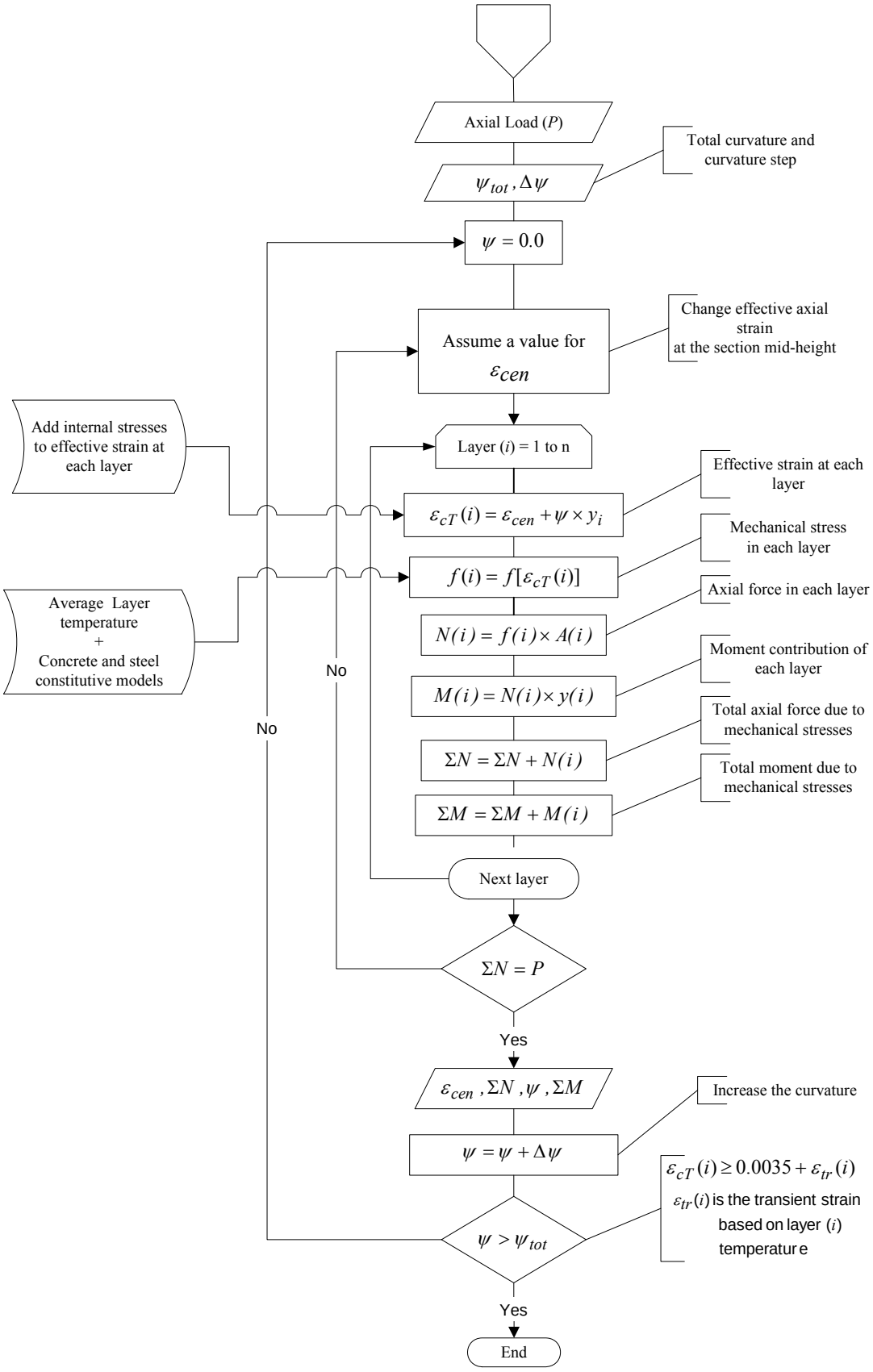

Fig. 10. Construction of moment-curvature diagram

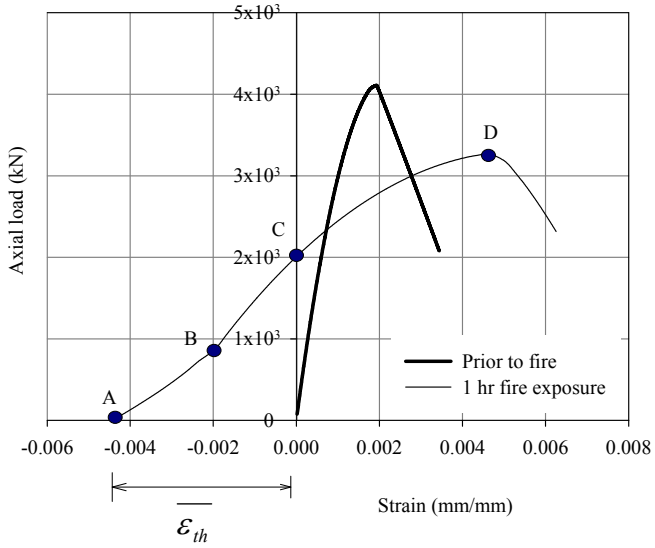

(a) Axial load-axial strain relationship

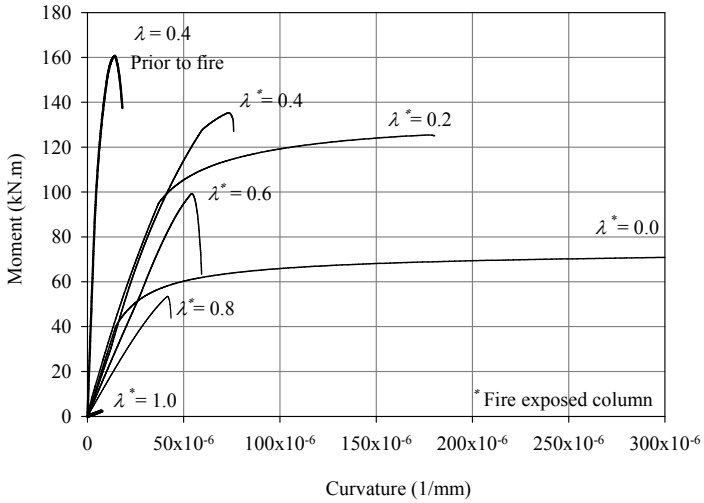

(b) Moment–curvature relationship

Fig. 11. Axial and flexural behaviour of example column

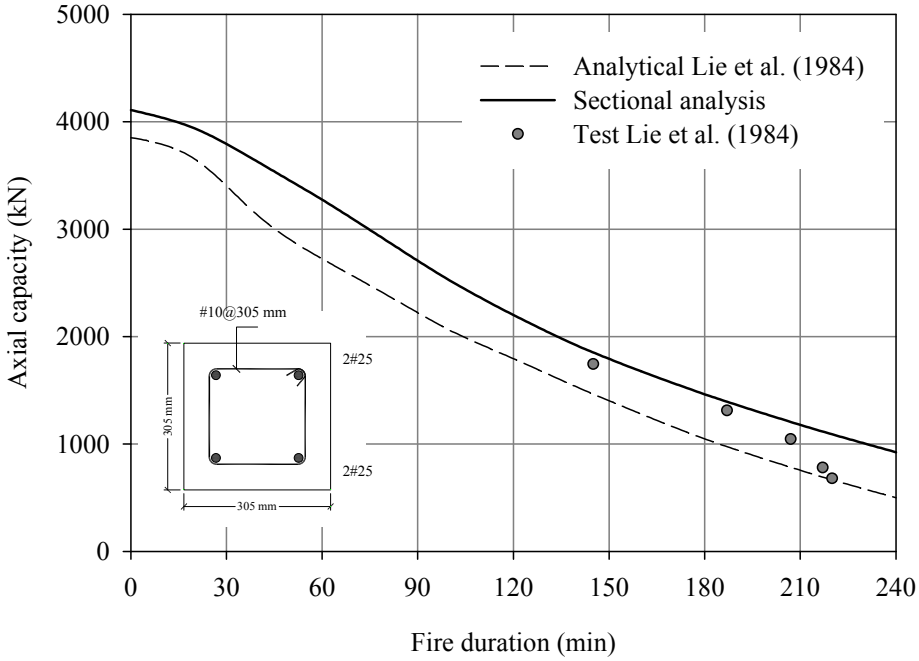

Fig. 12. Axial capacity-fire duration relationship

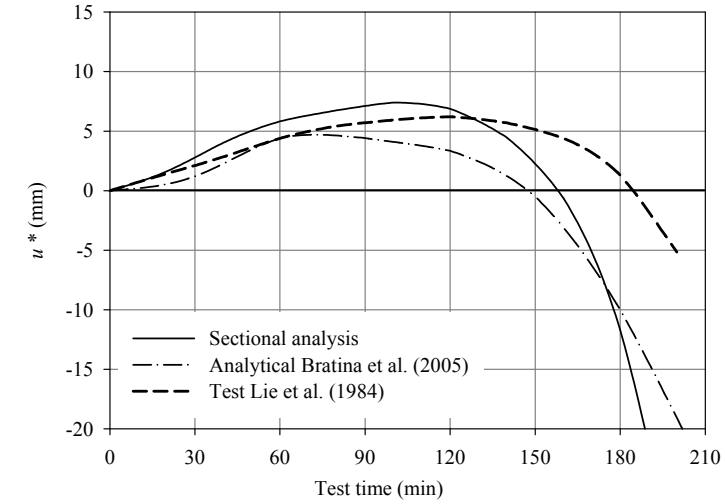

(a) P = 1067 kN

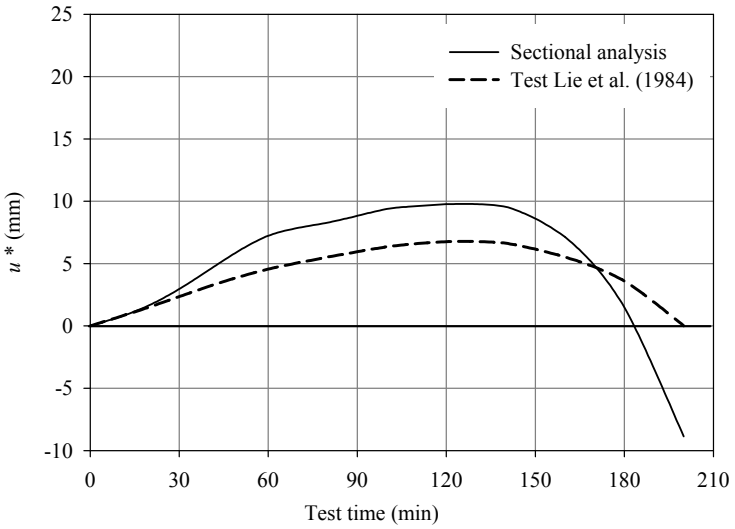

(b) P = 800 kN

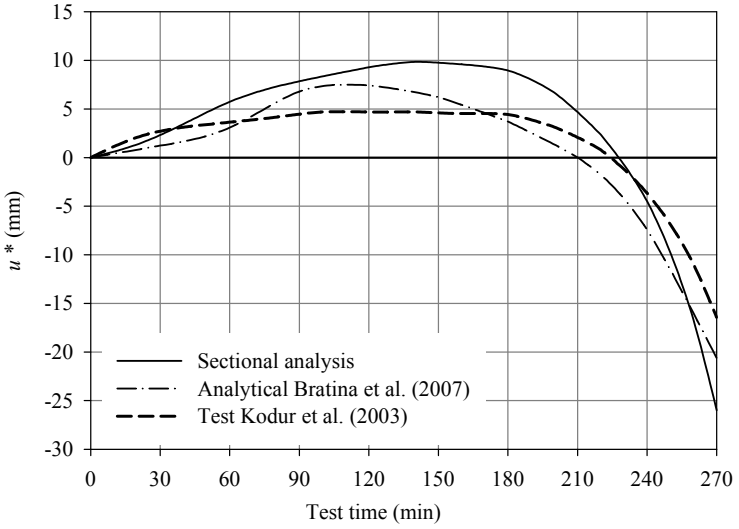

(c) P = 930 kN

Fig. 13. Axial deformation-fire duration relationship

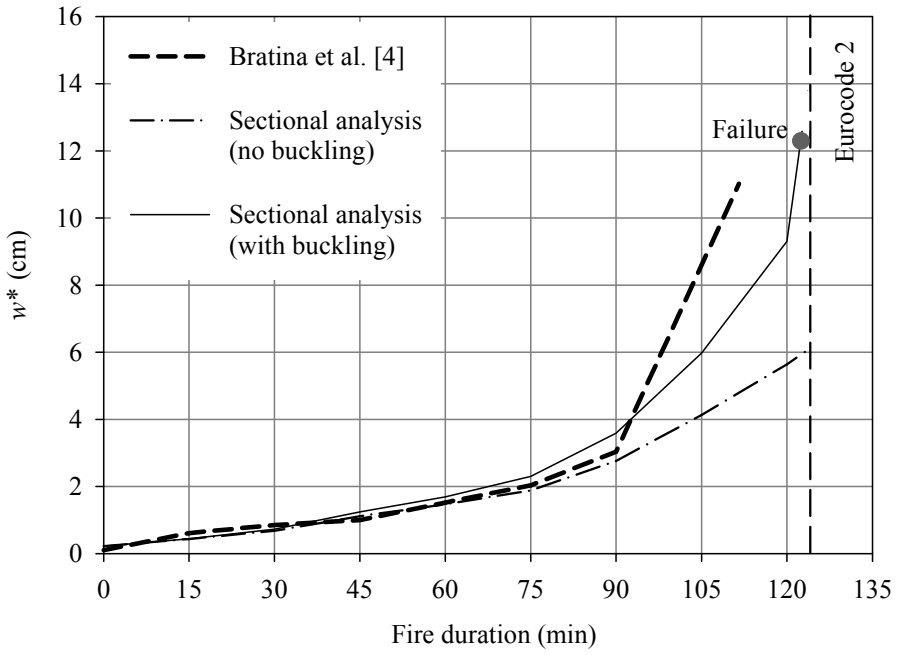

Fig. 14. Lateral deflection-fire duration relationship